

The rate of sea-level rise

Anny Cazenave^{1*}, Habib-Boubacar Dieng¹, Benoit Meyssignac¹, Karina von Schuckmann², Bertrand Decharme³ and Etienne Berthier¹

Present-day sea-level rise is a major indicator of climate change¹. Since the early 1990s, sea level rose at a mean rate of $\sim 3.1 \text{ mm yr}^{-1}$ (refs 2,3). However, over the last decade a slowdown of this rate, of about 30%, has been recorded^{4–8}. It coincides with a plateau in Earth's mean surface temperature evolution, known as the recent pause in warming^{1,9–12}. Here we present an analysis based on sea-level data from the altimetry record of the past ~ 20 years that separates interannual natural variability in sea level from the longer-term change probably related to anthropogenic global warming. The most prominent signature in the global mean sea level interannual variability is caused by El Niño–Southern Oscillation, through its impact on the global water cycle^{13–16}. We find that when correcting for interannual variability, the past decade's slowdown of the global mean sea level disappears, leading to a similar rate of sea-level rise (of $3.3 \pm 0.4 \text{ mm yr}^{-1}$) during the first and second decade of the altimetry era. Our results confirm the need for quantifying and further removing from the climate records the short-term natural climate variability if one wants to extract the global warming signal¹⁰.

Precisely estimating present-day sea-level rise caused by anthropogenic global warming is a major issue that allows assessment of the process-based models developed for projecting future sea level¹. Sea-level rise is indeed one of the most threatening consequences of ongoing global warming, in particular for low-lying coastal areas that are expected to become more vulnerable to flooding and land loss. As these areas often have dense populations, important infrastructures and high-value agricultural and bio-diverse land, significant impacts such as increasingly costly flooding or loss of freshwater supply are expected, posing a risk to stability and security^{17,18}. However, sea level also responds to natural climate variability, producing noise in the record that hampers detection of the global warming signal. Trends of the satellite altimetry-based global mean sea level (GMSL) are computed over two periods: the period 1994–2002 and the period 2003–2011 of the observed slowdown (Fig. 1a). GMSL time series from five prominent groups processing satellite altimetry data for the global ocean are considered (Methods). During recent years (2003–2011), the GMSL rate was significantly lower than during the 1990s (average of 2.4 mm yr^{-1} versus 3.5 mm yr^{-1}). This is observed by all processing groups (Fig. 1a). The temporal evolution of the GMSL rate (computed over five-year-long moving windows, starting in 1994 and shifted by one year) was nearly constant during the 1990s, whereas the rate clearly decreased by $\sim 30\%$ after ~ 2003 (Fig. 2a). This decreasing GMSL rate coincides with the pause observed over the last decade in the rate of Earth's global mean surface temperature increase^{9,10}, an observation exploited by

climate sceptics to refute global warming and its attribution to a steadily rising rate of greenhouse gases in the atmosphere. It has been suggested that this so-called global warming hiatus¹¹ results from El Niño–Southern Oscillation- (ENSO-) related natural variability of the climate system¹⁰ and is tied to La Niña-related cooling of the equatorial Pacific surface^{11,12}. In effect, following the major El Niño of 1997/1998, the past decade has favoured La Niña episodes (that is, ENSO cold phases, reported as sometimes more frequent and more intensive than the warm El Niño events, a sign of ENSO asymmetry¹⁹). The interannual (that is, detrended) GMSL record of the altimetry era seems to be closely related to ENSO, with positive/negative sea-level anomalies observed during El Niño/La Niña events². Recent studies have shown that the short-term fluctuations in the altimetry-based GMSL are mainly due to variations in global land water storage (mostly in the tropics), with a tendency for land water deficit (and temporary increase of the GMSL) during El Niño events^{13,14} and the opposite during La Niña^{15,16}. This directly results from rainfall excess over tropical oceans (mostly the Pacific Ocean) and rainfall deficit over land (mostly the tropics) during an El Niño²⁰ event. The opposite situation prevails during La Niña. The succession of La Niña episodes during recent years has led to temporary negative anomalies of several millimetres in the GMSL (ref. 15), possibly causing the apparent reduction of the GMSL rate of the past decade. This reduction has motivated the present study. From seasonal to centennial time scales, the two main contributions to GMSL variability and change come from ocean thermal expansion and ocean mass. Owing to water mass conservation in the climate system, sources of global ocean mass variations are land ice masses, land water storage and atmospheric water vapour content. Studies have shown that ENSO-driven interannual variability in the global water cycle strongly impacts land water storage^{12–15} and atmospheric water vapour²¹, hence ocean mass and GMSL. Here, we quantitatively estimate these interannual water mass contributions and remove them from the altimetry-based GMSL record, to isolate the longer-term signal caused by global warming (here, interannual refers to a temporal window in the range of one to five years, mainly ENSO-related, but not exclusively). To do this, two approaches are possible: estimate interannual land water storage plus atmospheric water vapour contributions; or directly estimate the interannual variability in global ocean mass. The Gravity Recovery and Climate Experiment (GRACE) space mission directly measures ocean mass and land water storage variations but only since ~ 2003 . Before GRACE, neither ocean mass nor land water storage variations can be directly computed from observations. However, the use of hydrological models developed for climate studies and water resource monitoring²² allows us to

¹Laboratoire d'Etudes en Géophysique et Océanographie Spatiales, 18 avenue E. Belin, 31400 Toulouse, France, ²Mediterranean Institute of Oceanography, avenue de l'Université, 83957 La Garde, France, ³Centre National de Recherches Météorologiques, MétéoFrance, 42 avenue G. Coriolis, 31100 Toulouse, France. *e-mail: anny.cazenave@legos.obs-mip.fr

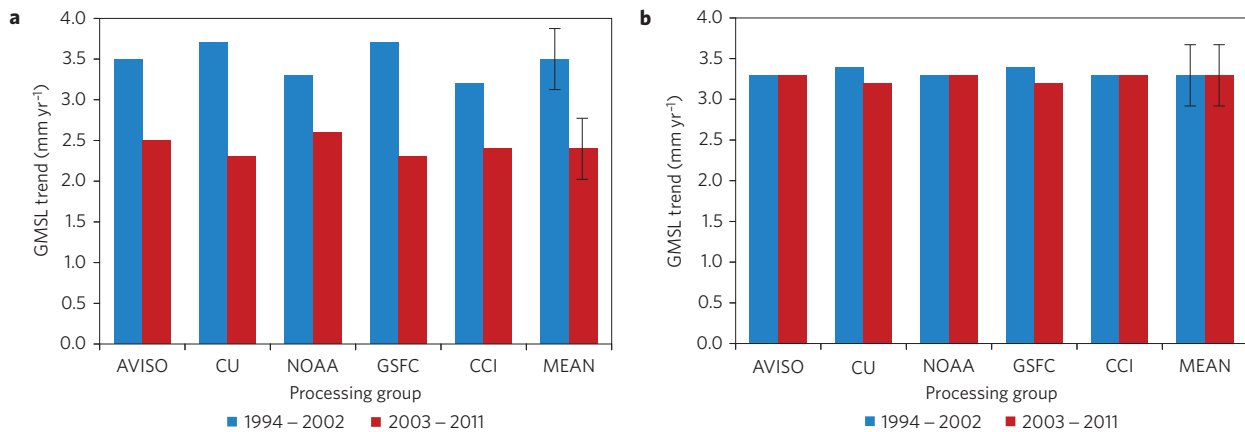


Figure 1 | GMSL trends during the 1994–2002 and 2003–2011 periods. **a**, GMSL trends computed over two time spans (January 1994–December 2002 and January 2003–December 2011) using satellite altimetry data from five processing groups (see Methods for data sources). The mean GMSL trend (average of the five data sets) is also shown. **b**, Same as **a** but after correcting the GMSL for the mass and thermosteric interannual variability (nominal case). Corrected means that the interannual variability due to the water cycle and thermal expansion are quantitatively removed from each original GMSL time series using data as described in the text. Black vertical bars represent the 0.4 mm yr⁻¹ uncertainty (ref. 2).

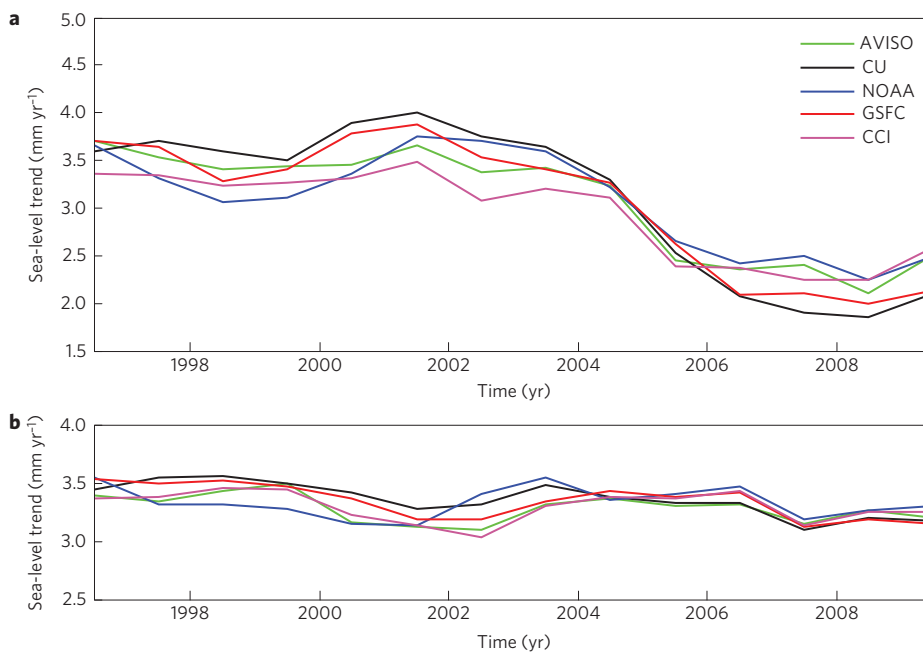


Figure 2 | GMSL rate over five-year-long moving windows. **a**, Temporal evolution of the GMSL rate computed over five-year-long moving windows shifted by one year (start date: 1994). **b**, Temporal evolution of the corrected GMSL rate (nominal case) computed over five-year-long moving windows shifted by one year (start date: 1994). GMSL data from each of the five processing groups are shown.

estimate the land water contribution since the beginning of the high-precision altimetry record. Both approaches are considered here. As a nominal case, we estimate the interannual land water contribution from a hydrological model (accounting for the atmospheric water vapour component) over the whole analysis time span (1994–2011). We also present as Supplementary Information three hybrid cases where the mass component is estimated as in the nominal case over 1994–2002 but replaced by GRACE data as of 2003. Data and models used to obtain the mass component are presented in the Methods and Supplementary Information. Detrended altimetry-based GMSL records and interannual mass components over the January 1994–December 2011 time span are shown in Fig. 3 (nominal case) and Supplementary Fig. 3 (hybrid case 1; in the following, figures shown as Supplementary Information correspond to hybrid case 1). As illustrated in Fig. 3 and Supplementary Fig. 3, the interannual

GMSL signal mainly (but not exclusively) results from ENSO-driven water mass redistributions among the climate system reservoirs, with strong positive and negative GMSL anomalies during the 1997/1998 El Niño and 2011 La Niña, respectively. This raises two questions: what is the impact of ENSO-related (or, more generally, interannual) variability on the estimation of the GMSL trend; and can we separate the interannual natural variability from the longer-term global warming trend in the GMSL record?

To answer these questions we subtracted the interannual mass and thermosteric components from the GMSL record. Although the short-term GMSL fluctuations are mostly related to the global water cycle (Fig. 3 and Supplementary Fig. 3), thermal expansion also slightly contributes. Thus we also removed short-term variations in thermal expansion from the GMSL record (see Methods for information about the ocean temperature data used to

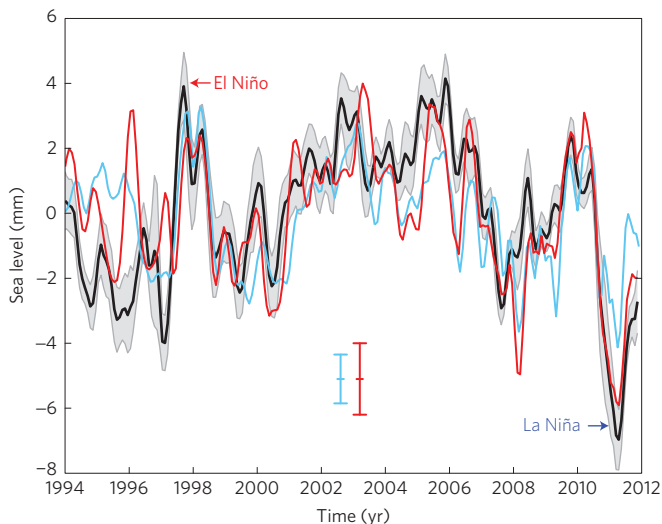


Figure 3 | Detrended GMSL, interannual mass and 'mass plus thermosteric' components. Black curve: mean detrended GMSL time series (average of the five satellite altimetry data sets) from January 1994–December 2011 and associated uncertainty (in grey; based on the dispersion of each time series around the mean). Light blue curve: interannual mass component based on the ISBA/TRIP hydrological model for land water storage plus atmospheric water vapour component over January 1994–December 2011. The red curve is the sum of the interannual mass and thermosteric components. This is the signal removed from the original GMSL time series (nominal case). Vertical bars represent the uncertainty of the monthly mass estimate (of 1.5 mm; refs 22,30; light blue bar) and monthly total contribution (mass plus thermosteric components; of 2.2 mm; refs 22,28–30; red bar).

compute thermal expansion and procedure applied to extract the corresponding interannual signal). Note that land ice also displays interannual mass variability¹. However, adequate data to quantify it globally and for the whole altimetry period are presently lacking. The sum of interannual mass plus thermosteric components is also shown in Fig. 3 and Supplementary Fig. 3, for both nominal and hybrid case 1. It is this signal that is removed from the GMSL record over the altimetry period. We recomputed the rate of the corrected GMSL time series over the same five-year-long moving windows (shifted by one year) as done previously. The temporal evolution of the corrected GMSL rate is shown in Fig. 2b and Supplementary Fig. 2b. The decreasing rate seen initially over the past decade has disappeared: the rate is now almost constant with time. Fig. 1b and Supplementary Fig. 1b show the corrected GMSL rates for the same two nine-year-long time spans as above, for each of the five altimetry data sets. The mean rate is also shown. The corrected mean rate now amounts to $3.3 \pm 0.1 \text{ mm yr}^{-1}$ over the two time intervals. The 0.1 mm yr^{-1} uncertainty is the formal error deduced from the dispersion around the mean. A more realistic uncertainty representing systematic errors affecting the altimetry-based GMSL rate (for example, owing to geophysical corrections applied to the altimetry data, and instrumental bias and drifts) would be rather closer to 0.4 mm yr^{-1} (ref. 2). However, this would not change our finding.

The result reported here shows that when removing from the GMSL time series the interannual variability mostly due to exchange of water between oceans, atmosphere and continents, with a smaller contribution from thermal expansion, there is no rate difference between the 1990s and the 2000s: the GMSL has almost linearly increased during the past 20 years. Although no GMSL acceleration is observed over this short time span, our result clearly advocates for no recent slowdown in global warming.

Although it has been suggested that several decades of satellite altimetry-based GMSL would be needed to isolate the long-term global warming signal⁶, our result also shows that this may be already achievable by removing the (mainly ENSO-driven) interannual variability, a procedure that enhances the signal-to-noise ratio, as previously shown for the Earth's global mean surface temperature evolution¹⁰. At present, a persistent positive energy imbalance between the amount of sunlight absorbed by Earth and the thermal radiation back to space is observed^{1,8,9,12,23}. The term missing energy⁹ is related to an apparent inconsistency between interannual variations in the net radiation imbalance inferred from satellite measurements and upper-ocean heating rate from *in situ* measurements⁹. Although progress has been achieved and inconsistencies reduced²⁴, the puzzle of the missing energy remains¹², raising the question of where the extra heat absorbed by the Earth is going^{9,12}. The results presented here will further encourage this debate as they underline the enigma between the observed plateau in Earth's mean surface temperature and continued rise in the GMSL. The larger GMSL rate calculated during the past decade than previously believed would be compatible with a significant warming contribution from the deep ocean. Such a possibility was raised by recent studies on the ocean heat content, suggesting that $\sim 30\%$ of the ocean warming has occurred below 700 m (ref. 25). This heat may be sequestered into the deep ocean during decades of large ocean–atmosphere natural variability²⁶, highlighting once more, as shown here, the role of short-term natural variability on longer-term change, probably associated with global warming.

Methods

Since the early 1990s, sea level has been routinely measured with quasi-global coverage and a few days/weeks revisit time by altimeter satellites: Topex/Poseidon (1992–2006), Jason-1 (2001–2013), Jason-2 (2008–), ERS-1 (1991–1996), ERS-2 (1995–2002), Envisat (2002–2011), Cryosat-2 (2010–) and SARAL/AltiKa (2013–). Altimetry-based GMSL time series are routinely produced by five processing groups: Archiving, Validation and Interpretation of Satellite Oceanographic Data (AVISO; www.aviso.oceanobs.com/en/news/ocean-indicators/mean-sea-level), Colorado University (CU; www.sealevel.colorado.edu/), Commonwealth Scientific and Industrial Research Organization (CSIRO; www.cmar.csiro.au/sealevel/sl_data_cmar.html), Goddard Space Flight Center (GSFC; podaac.jpl.nasa.gov/Integrated_Multi-Mission_Ocean_AltimetryData) and National Oceanographic and Atmospheric Administration (NOAA; ibis.drll.noaa.gov/SAT/SeaLevelRise/LSA_SLR_timeseries_global.php). The GMSL time series from these five groups are based on Topex/Poseidon, Jason-1/2 missions. Recently, in the context of the European Space Agency (ESA) Climate Change Initiative (CCI) Sea Level Project (www.esa-sealevel-cci.org), a new, improved product, combining the Topex/Poseidon, Jason-1/2 with the ERS-1/2 and Envisat missions, has been computed. At present, data up to December 2010 are available. Beyond that date, the CCI GMSL time series has been extended using the AVISO data. All products are considered here except the CSIRO one that uses older geophysical corrections for the Topex/Poseidon data. A small correction of -0.3 mm yr^{-1} is removed to each GMSL time series to account for the glacial isostatic adjustment effect (that is, the visco-elastic response of the solid Earth to the last deglaciation) on absolute sea level²⁷. Owing to known errors in the Topex/Poseidon altimetric system in the early part of the mission, we ignore the year 1993 when computing the GMSL trends.

To estimate the mass component due to global land water storage change, we use the Interaction Soil Biosphere Atmosphere (ISBA)/Total Runoff Integrating Pathways (TRIP) global hydrological model developed at MétéoFrance²². The ISBA land surface scheme calculates time variations of surface energy and water budgets in three soil layers. The soil water content varies with surface infiltration, soil evaporation, plant transpiration and deep drainage. ISBA is coupled with the TRIP module that converts daily runoff simulated by ISBA into river discharge on a global river channel network of 1° resolution. In its most recent version, ISBA/TRIP uses, as meteorological forcing, data at 0.5° resolution from the ERA Interim reanalysis of the European Centre for Medium-Range Weather Forecast (www.ecmwf.int/products/data/d/finder/parameter). Land water storage outputs from ISBA/TRIP are given at monthly intervals from January 1950 to December 2011 on a 1° grid (see ref. 22 for details). The atmospheric water vapour contribution has been estimated from the ERA Interim reanalysis. The land water storage and atmospheric water vapour contributions are further expressed in

equivalent sea level (ESL) through weighting by the ratio of the total land and Earth areas to the ocean area and multiplied by -1 . The land water plus atmospheric water vapour component was estimated over the January 1994–December 2011 time span.

Two thermal expansion data sets were considered: the V6.13 updated version of ocean temperature data down to 700 m, over January 1994–December 2006 (ref. 28) and Argo data down to 1,500 m over January 2007–December 2011 (ref. 29). As we focus on the interannual signal, we applied a high-pass filter (removing all signal >5 years) to the thermosteric time series. For the other data sets, a simple linear trend was removed (the ISBA/TRIP land water and atmospheric water vapour time series essentially display interannual variability; applying the high-pass filter or just removing a linear trend provides essentially the same results). The time series are estimated at monthly time steps. Annual and semi-annual signals are removed by fitting 12- and 6-month period sinusoids to each time series (using a climatology produces similar results). A four-month running mean smoothing is further applied to all time series. Errors in land surface modelling are generally mainly due to uncertainties in atmospheric forcing than in physical parameterizations such as the representation of groundwater dynamics or not³⁰. The global ISBA/TRIP simulation used here was extensively evaluated and the simulated global land water storage was found very close to the GRACE signal over their overlapping time span²². Errors of associated monthly mass component are estimated to 1.3–1.5 mm ESL (refs 22,30). Errors on monthly water vapour component are <0.5 mm ESL. Errors on monthly thermosteric values are estimated to ~ 1.4 mm ESL (refs 28,29).

In Figs 1–3, the mass component is based on ISBA/TRIP plus water vapour over the whole 1994–2011 time span (nominal case). Supplementary Figs 1, 2 and 3 use ISBA/TRIP outputs plus water vapour over 1994–2002 and GRACE data for 2003–2011 (hybrid case 1). In both cases, thermosteric data are from ref. 28 over 1994–2006 and Argo for 2007–2011.

Received 16 October 2013; accepted 4 February 2014;
published online 23 March 2014

References

1. IPCC *Climate Change 2013: The Physical Science Basis* (eds Stocker, T. F. et al.) (Cambridge Univ. Press, 2013).
2. Nerem, R. S., Chambers, D. P., Choe, C. & Mitchum, G. T. Estimating mean sea level change from the TOPEX and Jason altimeter missions. *Mar. Geodesy* **33**, 435–446 (2010).
3. Church, J. A. & White, N. J. Sea-level rise from the late 19th to the early 21st century. *Surveys Geophys.* **32**, 585–602 (2011).
4. Willis, J. K., Chambers, D. P. & Nerem, R. S. Assessing the globally averaged sea level budget on seasonal to interannual time scales. *J. Geophys. Res.* <http://dx.doi.org/10.1029/2007jc004517> (2008).
5. Leuliette, E. W. & Miller, L. Closing the sea level rise budget with altimetry, Argo and GRACE. *Geophys. Res. Lett.* **36**, L04608 (2009).
6. Leuliette, E. W. & Willis, J. K. Balancing the sea level budget. *Oceanography* **24**, 122–129 (2011).
7. Chen, J. L., Wilson, C. R. & Tapley, B. D. Contribution of ice sheet and mountain glacier melt to recent sea level rise. *Nature Geosci.* **6**, 549–552 (2013).
8. Hansen, J., Sato, M., Kharecha, P. & von Schuckmann, K. Earth's energy imbalance and implications. *Atmos. Chem. Phys.* **11**, 13421–13449 (2011).
9. Trenberth, K. E. & Fasullo, J. T. Tracking Earth's energy. *Science* **328**, 316–317 (2010).
10. Foster, G. & Rahmstorf, S. Global temperature evolution 1979–2010. *Environ. Res. Lett.* **6**, 044022 (2011).
11. Kosaka, Y. & Xie, S.-P. Recent global warming hiatus tied to equatorial Pacific surface cooling. *Nature* **501**, 403–407 (2013).
12. Trenberth, K. E. & Fasullo, J. T. An apparent hiatus in global warming? *Earth's Future* <http://dx.doi.org/10.1002/2013EF000165> (2013).
13. Llovel, W. et al. Terrestrial waters and sea level variations on interannual time scale. *Glob. Planet. Change* **75**, 76–82 (2011).
14. Cazenave, A. et al. ENSO influence on the global mean sea level over 1993–2010. *Mar. Geodesy* **35**, 82–97 (2012).
15. Boening, C., Willis, J. K., Landerer, F. W. & Nerem, R. S. The 2011 La Niña: So strong, the oceans fell. *Geophys. Res. Lett.* **39**, L19602 (2012).
16. Fasullo, J. T., Boening, C., Landerer, F. W. & Nerem, R. S. Australia's unique influence on global sea level in 2010–2011. *Geophys. Res. Lett.* **40**, 4368–4373 (2013).
17. Nicholls, R. J. & Cazenave, A. Sea-level rise and its impact on coastal zones. *Science* **328**, 1517–1520 (2010).
18. Hallegatte, S., Green, C., Nicholls, R. J. & Corfee-Morlot, J. Future flood losses in major coastal cities. *Nature Clim. Change* **3**, 802–806 (2013).
19. Gergis, J. L. & Fowler, A. M. A history of ENSO events since A.D. 1525: Implications for future climate change. *Climatic Change* **92**, 343–387 (2009).
20. Gu, G. & Adler, R. F. Precipitation and temperature variations on the interannual time scale: Assessing the impact of ENSO and volcanic eruptions. *J. Climate* **24**, 2258–2270 (2011).
21. Trenberth, K., Fasullo, J. & Smith, L. Trends and variability in column-integrated atmospheric water vapor. *Clim. Dynam.* **24**, 741–758 (2005).
22. Alkama, R. et al. Global evaluation of the ISBA-TRIP continental hydrological system. Part 1: Comparison to GRACE Terrestrial Water Storage estimates and in-situ river discharges. *J. Hydromet.* **11**, 583–600 (2010).
23. Church, J. A. et al. Revisiting the Earth's sea-level and energy budgets from 1961 to 2008. *Geophys. Res. Lett.* <http://dx.doi.org/10.1029/2011gl048794> (2011).
24. Loeb, G. N. et al. Observed changes in top-of-the-atmosphere radiation and upper-ocean heating consistent within uncertainty. *Nature Geosci.* **5**, 110–113 (2012).
25. Balmaseda, M. A., Trenberth, K. & Kallen, E. Distinctive climate signals in reanalysis of global ocean heat content. *Geophys. Res. Lett.* **40**, 1–6 (2013).
26. Meehl, G. A., Arblaster, J. M., Fasullo, J. T., Hu, A. & Trenberth, K. E. Model based evidence of deep-ocean heat uptake during surface-temperature hiatus periods. *Nature Clim. Change* **1**, 360–364 (2011).
27. Peltier, W. R. Global glacial isostasy and the surface of the ice-age Earth: The ICE-5G (VM2 model and GRACE). *Annu. Rev. Earth Planet. Sci.* **32**, 111–149 (2004).
28. Ishii, M. & Kimoto, M. Reevaluation of historical ocean heat content variations with time-varying XBT and MBT depth bias corrections. *J. Oceanogr.* **65**, 287–299 (2009).
29. Von Schuckmann, K. & Le Traon, P. Y. How well can we derive global ocean indicators from Argo data? *Ocean Sci.* **7**, 783–791 (2011).
30. Vergnes, J.-P. & Decharme, B. A simple groundwater scheme in the TRIP river routing model: Global off-line evaluation against GRACE terrestrial water storage estimates and observed river discharges. *Hydrol. Earth Syst. Sci.* **16**, 3889–3908 (2012).

Acknowledgements

This work was supported by CNES, CNRS, MétéoFrance, The University of Toulon and the ESA CCI project.

Author contributions

A.C. conceived the study and wrote the article. H.-B.D. conducted the calculations. B.D. and K.v.S. provided the ISBA/TRIP and Argo data, respectively. B.M. and E.B. contributed to the interpretation and discussion.

Additional information

Supplementary information is available in the online version of the paper. Reprints and permissions information is available online at www.nature.com/reprints. Correspondence and requests for materials should be addressed to A.C.

Competing financial interests

The authors declare no competing financial interests.